Received: 17 February 2021 | Revised: 1 November 2021 | Accepted: 5 January 2022

DOI: 10.1002/jbt.23018

WILEY

Potential thiosemicarbazone-based enzyme inhibitors: Assessment of antiproliferative activity, metabolic enzyme inhibition properties, and molecular docking calculations

Hasan Yakan[1] | Ümit M. Koçyiğit[2] | Halit Muğlu[3] | Mustafa Ergul[2] | Sultan Erkan[4] | Emre Güzel[5,6] | Parham Taslimi[7,8] | İlhami Gülçin[9]

[1]Department of Science and Mathematics Education, Ondokuz Mayıs University, Samsun, Turkey

[2]Department of Basic Pharmaceutical Sciences, Sivas Cumhuriyet University, Sivas, Turkey

[3]Department of Chemistry, Kastamonu University, Kastamonu, Turkey

[4]Department of Chemistry, Sivas Cumhuriyet University, Sivas, Turkey

[5]Department of Engineering Fundamental Sciences, Sakarya University of Applied Sciences, Sakarya, Turkey

[6]Biomedical Technologies Application and Research Center (BIYOTAM), Sakarya University of Applied Sciences, Sakarya, Turkey

[7]Department of Biotechnology, Faculty of Science, Bartin University, Bartin, Turkey

[8]Department of Chemistry, Faculty of Science, İstinye University, İstanbul, Turkey

[9]Department of Chemistry, Faculty of Science, Atatürk University, Erzurum, Turkey

Correspondence

Hasan Yakan, Department of Science and Mathematics Education, Ondokuz Mayıs University, 55270 Samsun, Turkey.
Email: hasany@omu.edu.tr

Ümit M. Koçyiğit, Department of Basic Pharmaceutical Sciences, Sivas Cumhuriyet University, 58140 Sivas, Turkey.
Email: ukocyigit@cumhuriyet.edu.tr

Funding information

Scientific Research Project Fund of Sivas Cumhuriyet University,
Grant/Award Numbers: ECZ079, RGD-020

Abstract

A new series of thiosemicarbazone derivatives (**1**–**11**) were prepared from various aldehydes and isocyanates with high yields and practical methods. The structures of these compounds were elucidated by Fourier transform infrared, ^{1}H-nuclear magnetic resonance (NMR), ^{13}C-NMR spectroscopic methods and elemental analysis. Cytotoxic effects of target compounds were determined by 2,3-bis-(2-methoxy-4-nitro-5-sulfophenyl)-2H-tetrazolium-5-carboxanilide assay and compound **1** showed significant cytotoxic activity against both MCF-7 and MDA-MB-231 cells, with half-maximal inhibitory concentration values of 2.97 µM and 6.57 µM, respectively. Moreover, in this study, the anticholinergic and antidiabetic potentials of these compounds were investigated. To this aim, the effect of the newly synthesized thiosemicarbazone derivatives on the activities of acetylcholinesterase (AChE) and αglycosidase (α-Gly) was evaluated spectrophotometrically. The title compounds demonstrated high inhibitory activities compared to standard inhibitors with K_i values in the range of 122.15–333.61 nM for α-Gly (K_i value for standard inhibitor = 75.48 nM), 1.93–12.36 nM for AChE (K_i value for standard inhibitor = 17.45 nM). Antiproliferative activity and enzyme inhibition at the molecular level were performed molecular docking studies for thiosemicarbazone derivatives. 1M17, 5FI2, and 4EY6, 4J5T target proteins with protein data bank identification with (**1**–**11**) compounds were docked for anticancer and enzyme inhibition, respectively.

KEYWORDS

antiproliferative activity, enzyme inhibition, molecular docking, Schiff base, thiosemicarbazone

1 | INTRODUCTION

Thiosemicarbazones are an important class of organic chemistry with similar biological and medicinal effects. They have been reported having numerous medicinal and biological activities such as antibacterial,[1,2] antioxidant,[3–5] antimicrobial,[6] anti-inflammatory,[7] anticancer,[8,9] antituberculosis,[10] enzyme inhibition,[11] cytotoxicity and antifungal activity.[12,13]

Acetylcholinesterase (E.C.3.1.1.7, AChE, acetylhydrolase) is an enzyme from the hydrolase group that hydrolyzes the neurotransmitter acetylcholine. AChE is mainly found at the neuromuscular junction and cholinergic brain synapses where it terminates the synaptic transmission. It belongs to the carboxylesterase family of enzymes.[14–16] It has been observed that the activity of AChE is increased in the cortex and hippocampus in Alzheimer's brains, while the amount and activation of acetylcholine decreases.[17–19] With the knowledge that the factors causing Alzheimer's disease (AD) are not known precisely, preventive treatments have not been found fully today. However, symptomatic treatments that slow down the course of the disease or delay its progression have been tried and tried. Acetylcholinesterase inhibitors (AChEi), which are cholinergic agents, are the most effective and specific approach in drug treatment used for the improvement of symptoms of AD.[17,20] However, none of the current AChEi drugs have been fully successful.[14] Nonetheless, in recent years, some 1,3,4-thiadiazole hybrid compounds presented for acetylcholinesterase enzyme inhibitory and showed promising activities against AChE.[21]

α-Glycosidase enzymes are located on the brushy surface of the small intestine. They are responsible for breaking down complex carbohydrates. These enzymes break down oligo- and disaccharides into monosaccharides.[22] Monosaccharides are easily absorbed from the intestinal wall and pass into the blood. α-glycosidase enzyme inhibitors inhibit these enzymes competitively. Glucoamylase, sucrase, maltase, isomaltase, and lactase are known as important α-glycosidase enzymes.[23] The effects of α-glycosidase enzyme inhibitors on these enzymes are different. The net result of enzyme inhibition in carbohydrate absorption is a delay. This delay does not cause malabsorption. In addition to delaying carbohydrate absorption, α-glycosidase enzyme inhibitors may also alter the gastrointestinal hormonal axis.[24,25] α-Glycosidase enzyme inhibitors are acarbose (ACR), voglibose, and miglitol. ACR is a nitrogen-containing pseudotetrasaccharide.[24]

The most important side effects belong to the gastrointestinal system carbohydrates that cannot be digested in the small intestine are metabolized by bacteria in the colon. This fermentation of undigested carbohydrates causes complaints of bloating, abdominal pain, diarrhea, and gas.[26] These side effects are dose-related. Therefore, when starting with very low doses and increasing slowly, the side effect profile will be narrower. It was observed that some of the complaints of the patients who had such complaints at the beginning disappeared while continuing the medication.[25] Liver enzyme disorders may occur in patients using high doses of medication. Drug-induced hypoglycemia does not occur. However, in combination therapies, hypoglycemia may occur depending on the effect of the other drug. Docking applications are frequently used in drug modeling and development studies. Docking simulations take place at the molecular level. Thus, information can be gathered up to the type of secondary chemical interaction with target proteins representing the cell line of the drug active agent. Besides this, binding modes are obtained in three dimensions. The difference between the interaction types and energies of a series of drug candidate molecules can be easily distinguished.[27]

In the present study, we describe the synthesis, structure characterization, evaluation of novel thiosemicarbazone derivatives (**1–11**) as effective anticancer agents and carbonic anhydrase enzyme inhibitors (Scheme 1). Moreover, we examine the activity with the revealed metabolic enzymes of studied molecules by molecular docking studies.

2 | MATERIALS AND METHODS

2.1 | Instruments and chemicals

All reagents and solvents were bought in Sigma-Aldrich, Acros Organics, or Merck Chemical Company and were used without further purification. The solvents were of spectroscopic grade. A Stuart Melting Point 30 apparatus was used to determine melting points and uncorrected. The elemental analysis was performed on a Eurovector EA3000-Single. A Bruker Alpha Fourier transform infrared spectroscopy (FT-IR) spectrometer was used to record infrared spectra. ^{1}H and ^{13}C nuclear magnetic resonance (NMR) spectra were taken on a Bruker Avance DPX-400 spectrophotometer (400 MHz) in dimethyl sulfoxide (DMSO)-d_6.

2.2 | Synthesis of thiosemicarbazone derivatives including Schiff base (1–11)

To a solution of various isothiocyanates (7.0 mmol) and hydrazine monohydrate (7.0 mmol) in ethanol (20 ml) was added dropwise with vigorous stirring and cooling in an ice bath. The reaction mixture was kept in a refrigerator overnight. The resulting precipitate was filtered, dried, and purified with ethanol to afford thiosemicarbazides. Then, formed thiosemicarbazides (4 mmol), different aldehydes (4 mmol), and one drop of HCl were added to aqueous ethanol (20 ml) and the mixture was refluxed at 78°C for 3–5 h. The resultant solid was filtered, washed, and dried in air. The compounds were successfully prepared with good yields (60%–88%) as shown in Scheme 2.

2.3 | Cell culture

Human breast cancer cell lines MCF-7 (HTB-22) and MDA-MB-231 (HTB-26) were purchased from American Type Culture Collection and maintained in Dulbecco's modified Eagle's medium (DMEM;

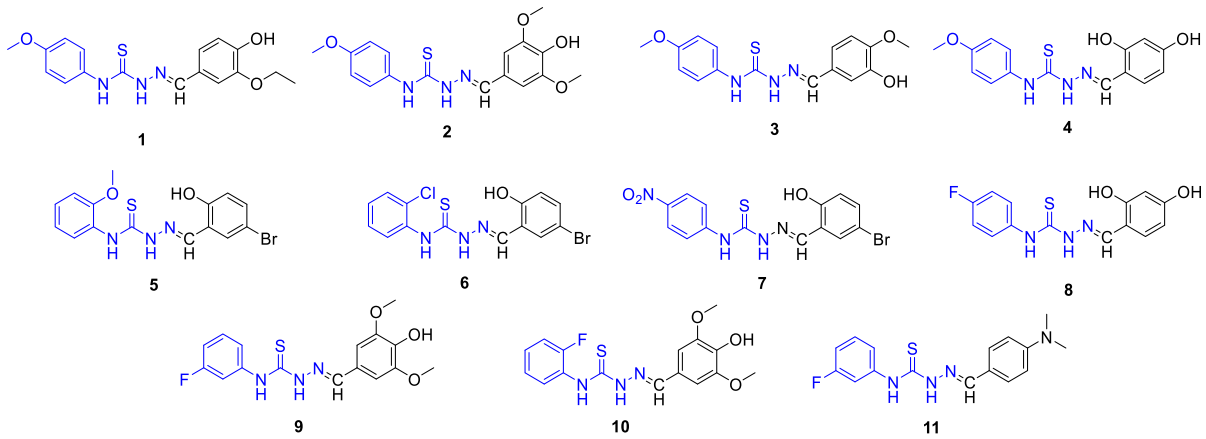

SCHEME 1 Chemical structures of thiosemicarbazone derivatives (**1**–**11**)

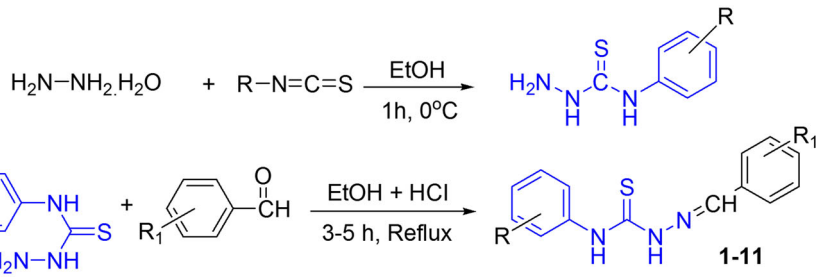

Compound	R	R_1	Compound	R	R_1
1	4-OCH_3	3-OC_2H_5-4-OH	**7**	4-NO_2	2-OH-5-Br
2		3,5-diOCH_3-4-OH	**8**	4-F	2,4-diOH
3		3-OH-4-OCH_3	**9**	3-F	3,5-diOCH_3-4-OH
4		2,4-diOH	**10**	2-F	3,5-diOCH_3-4-OH
5	2-OCH_3	2-OH-5-Br	**11**	3-F	4-*N*,*N*′diCH$_3$
6	2-Cl	2-OH-5-Br			

SCHEME 2 Synthesis route of thiosemicarbazone derivatives (**1**–**11**)

Sigma-Aldrich) supplemented with 10% fetal bovine serum (Sigma-Aldrich), 1% L-glutamine (Sigma-Aldrich), and 1% penicillin/streptomycin (Sigma-Aldrich). The cells were incubated at 37°C and in a 5% CO_2 humidified atmosphere. Cisplatin was used as a positive control and was obtained from Sigma-Aldrich. All compounds and cisplatin were dissolved in DMSO and 10 mM stock solutions were prepared. The stock solutions were diluted with DMEM before the applications, as the final concentration of DMSO did not exceed 0.5%.

2.4 | Cell viability assay

`Cytotoxicity of the synthesized compounds and cisplatin was determined using the 2,3-bis-(2-methoxy-4-nitro-5-sulfophenyl)-2H-tetrazolium-5-carboxanilide (XTT) assay (Roche Diagnostic). Breast cancer cells were plated in 96-well plates (Corning) at a density of 1×10^4 cells per well in 100 µl culture media mix and were allowed to attach overnight before treatment. The cells were then exposed to the compounds and cisplatin at 0.1, 5, 10, 25, 50, and 100 µM concentrations for 24 h. At the end of the incubation, DMEM was aspirated and the wells were washed two times with phosphate-buffered saline. Afterward, 100 µl DMEM without phenol red and a mixture of 50 µl XTT labeling solution were added to each well, and then the plates were incubated at 37°C for 4 h. The plates were shaken and the absorbances were determined using an enzyme-linked immunosorbent assay microplate reader (Thermo Fisher Scientific) at 450 nm.[28] All experiments were performed in triplicate and the cell viability was expressed as viable cell amount percent compared to control, as untreated cells. The half-maximal inhibitory concentration (IC_{50}) values of the compounds in MCF-7 and MDA-MB-231 cell lines were calculated by Graph Prism 7 software (GraphPad Software, Inc).

2.5 | Enzyme studies

2.5.1 | Determination of antidiabetic potential

To determine the antidiabetic potential of new thiosemicarbazone derivatives, the effects of these molecules on the α−glycosidase enzyme were investigated by the spectrophotometric method. The inhibitory potential of the new thiosemicarbazone derivatives on the α-glycosidase (α-Gly) enzyme was implemented using *p*-nitrophenyl-D-glucopyranoside (*p*-NPG) as described in the previous study.[29] For this, an enzyme solution (20 µl) and sample (10–100 µl) were mixed in 100 µl buffer (pH 7.4). Different solutions were prepared to determine the best enzyme inhibitor concentration. After that, *p*-NPG was added to the start of the reaction at 35°C and the sample was incubated at the same temperature for 12 min. Absorbances were monitored at 405 nm. Finally, Lineweaver Burk plots were used to determine other inhibition parameters such as V_{max} and K_i.[30]

2.5.2 | Determination of anti-AD potential

To determine the anticholinergic potentials of the newly synthesized thiosemicarbazone derivatives, the effect of these molecules on the AChE enzyme activity was determined spectrophotometrically using the Ellman method.[31] In the Ellman method, acetylthiocholine, which is a thiol ester, is used as the substrate instead of acetylcholine, which is the oxy ester. According to the principle of the Ellman method, acetylthiocholine is hydrolyzed by AChE and the thiocholine released as a result of hydrolysis reacts with the Ellman reagent 5,5′-dithio-bis-(2-nitrobenzoic acid). As a result of the reaction, the yellow chromophore 5-thio-2-nitrobenzoic acid is formed. The rate of formation (intensity of color) of this yellow-colored compound formed at the end of the reaction is determined by measuring the absorbance at 412 nm.[31] The intensity of this yellow color is directly proportional to the AChE enzyme activity.[32]

Studies on the determination of IC_{50} values for inhibitors: For thiosemicarbazone derivatives, their activities at different inhibitor concentrations were measured and their graphs were drawn as % activity - [I], and IC_{50} values were calculated from the equation of the curve.[31]

2.6 | Molecular docking studies

In recent years, in silico studies have played an active role in drug design. Molecular docking is a complex process with many steps. In this process, after the ligand and protein are optimized, the active site of the target protein is determined with the most suitable rigid receptor docking method. This process is a very complicated step. Because the amino acid side chains are kept immobile in the active site and the joining is ensured in the appropriate poses to ensure the most appropriate coupling. In silico work was carried out with Maestro 12.6 software (Schrodinger Suite Program).[25,33] 1M17 target protein containing the epidermal growth factor receptor tyrosine kinase domain was used for the antiproliferative effect of my newly synthesized drug candidate molecules against the MCF-7 cell line.[34] 5FI2 target protein suitable for the MDA-MB-231 cell line structure was preferred. 5FI2 represents the crystal structure of human glutaminase C (GAC). This target protein contains the enzymatic activity of GAC and the molecular structure capable of inhibiting the low nanomolar (nM) potency triple-negative MDA-MB-231 breast cancer growth.[35] 4EY6 target protein, which is the crystal structure of recombinant AChE, and 4J5T target protein, which is the crystal structure of α-glucosidase I, were preferred for enzyme inhibition effect.[36,37]

3 | RESULTS

3.1 | Physical and structural evaluations

The results for the physical properties, yields, melting points, and elemental analyses are given in Tables S1 and S2. In the FT-IR spectra of all the compounds, the asymmetric and symmetric stretching peaks of the amino group (–NH_2) of thiosemicarbazide were not observed at 3450–3250 cm^{-1}. The signal of the aldehyde group (–CHO) of the starting material was not observed at 2780–2660 cm^{-1}. Besides, the characteristic C=N stretching vibration of imines was shown at around 1560–1510 cm^{-1} as new peak. For compounds **1–11**, the amino peaks (–NH) of the thiosemicarbazide region were observed at 3341–3115 cm^{-1}, respectively. The thiocarbonyl group signals (–C=S) of the thiosemicarbazide region were observed at 1468–1407 cm^{-1}. In compounds **1–10**, the –OH stretching vibrations of phenolic aldehydes were observed at 3527–3337 cm^{-1}. The asymmetric and symmetric stretching peaks of the nitro group (–NO_2) were observed at 1502 and 1261 cm^{-1} for compound **7**. In compounds **5–7**, Ar–Br vibration signals were observed at 626, 682, and 693 cm^{-1}, respectively (see Figures S1–S11). These vibration values of the obtained molecules are consistent with similar compounds in the literature.[38,39] The frequency data were given in Table S3.

The ^{1}HNMR spectra of the compounds were taken in DMSO-d_6; the chemical shifts are given in Table S4. Signals of DMSO-d_6 and water in DMSO (HOD, H_2O) were observed around 2.00, 2.55 (quintet), and 3.40 (variable, depending on the solvent and its concentration) ppm, respectively. For compounds **1–11**, the amino peaks (–NH) of the thiosemicarbazide region were observed as a singlet at 12.17–9.83 ppm. The imin (–CH=N) peaks of all the compounds were observed as a singlet at 8.48–8.03 ppm. The OH signals of the compounds were detected as a singlet at 10.41–8.89 ppm except for compound **11** (see Figures S12–S22). The aromatic protons (H1–H5) of the aniline ring were observed at 8.27–6.90 ppm for all compounds. For compounds **1–5**, the proton signals of the methoxy group (–OCH_3) of the aniline region showed as a singlet at 3.77, 3.77, 3.77, 3.76, and 3.91 ppm, respectively. In compounds **2**, **3**, **9**, and

TABLE 1 IC_{50} values of the synthesized compounds against breast cancer MCF-7 and MDA-MB-231 cell lines

Compounds	*R*	R_1	MCF-7	MDA-MB-231
1	4-OCH_3	3-OC_2H_5-4-OH	2.97	6.57
2	4-OCH_3	3,5-diOCH_3-4-OH	68.91	73.85
3	4-OCH_3	3-OH-4-OCH_3	57.14	65.14
4	4-OCH_3	2,4-diOH	13.76	19.32
5	2-OCH_3	2-OH-5-Br	5.83	7.24
6	2-Cl	2-OH-5-Br	7.97	8.21
7	4-NO_2	2-OH-5-Br	3.22	7.13
8	4-F	2,4-diOH	11.09	16.73
9	3-F	3,5-diOCH_3-4-OH	73.21	88.96
10	2-F	3,5-diOCH_3-4-OH	69.78	68.17
11	3-F	4-*N*,*N*′-diCH_3	12.53	14.74
Cisplatin			27.9	33.7

Note: The cells were exposed to various concentrations of the compounds ranging between 0.1 to 100 μM and the cytotoxicity was examined using the XTT assay.

Abbreviations: IC_{50}, half-maximal inhibitory concentration; XTT, 2,3-bis-(2-methoxy-4-nitro-5-sulfophenyl)-2H-tetrazolium-5-carboxanilide.

10, the proton signals of the methoxy group (–OCH_3) showed as a singlet at 3.83, 3.82, 3.84, and 3.82 ppm, respectively. These consequences are consistent with reported values for similar compounds.[38–40]

The ^{13}C NMR spectra of the obtained molecules were taken in DMSO-d_6 (heptet peaks, 39–41 ppm) and the chemical shifts are summarized in Table S5. All the compounds (**1–11**), the –C═S peaks (–NH) of the thiosemicarbazide region were observed at 177.3–175.0 ppm. The characteristic –C═N peaks of imine were detected at 152.1 and 137.6 ppm for all compounds (see Figures S23–S33). In the compounds (**1–11**), the aromatic carbon atom signals of the aniline region (C1–C6) were resonated between 163.2 and 102.7 ppm, and those from the aldehydic ring (C7–C12) were detected 161.2–102.7 ppm. Moreover, in compounds **1–4**, **7**, and **8**, the signals of the carbon (for C1) were shifted downfield (high values of δ) relative to the signal of benzene (128.5 ppm) due to the presence of the 4-OCH_3, 4-NO_2, and 4-F groups. It was observed at 157.5, 157.5, 157.3, 157.2, 144.3, and 162.5 ppm, respectively. Similarly, in compounds **1–4**, and **8–11**, the signals of the carbon (for C10) were shifted downfield (high values of δ) relative to the signal of benzene (128.5 ppm) due to the presence of 4-OH (147.7 ppm), 4-OH (138.5 ppm), 4-OCH_3 (150.2 ppm), 4-OH (158.6 ppm), 4-OH (158.7 ppm), 4-OH (138.7 ppm), 4-OH (138.6 ppm), 4-$N(CH_3)_2$ (160.8 ppm) atoms/groups. Besides this, in Compounds **8–11**, the C atoms (for C1–C6) were also split into doublets owing to interacting with the atomic nucleus of F. These consequences are consistent with re–ported values for similar compounds.[38,41,42]

3.2 | Antiproliferative activity

In the literature, many studies have shown the anticancer effects of thiosemicarbazide derivatives against several cancer cells. In this study, antiproliferative activities of all newly synthesized compounds were evaluated against MCF-7 and MDA-MB-231 cell lines using the XTT assay. Cisplatin is used as positive control and the IC_{50} values of the compounds are given in Table 1. As shown in Table 1, except for compounds **2**, **3**, **9**, and **10**, all of the other compounds showed higher cytotoxicity than cisplatin in both cell lines. Moreover, the compounds exhibited the most cytotoxic activities on MCF-7 cells when compared to MDA-MB-231 cells. Among the compounds, compound **1** exhibited the most potent cytotoxic activity with 2.97 and 6.57 μM IC_{50} values on MCF-7 and MDA-MB-231 cell lines, respectively. When Table 1 is examined, the aniline region does almost not affect cytotoxic activity. For instance, compounds **2**, **9**, and **10**, although there are different groups of the aniline region 4-OCH_3, 3-F, and 2-F, respectively, these compounds have the lowest cytotoxic activity. Therefore, the aldehydic region of the compounds affects cytotoxic activity more, and these three compounds involve 3,5-diOCH_3-4-OH substituents. When we look at compounds **1–4**, the aniline region of these compounds has a 4-OCH_3 group. Although compound **1** exhibits the highest cytotoxic activity, compounds **2–4** show lower activity. Moreover, the aldehydic regions of compounds **5–7** possess 2-OH-5-Br substituents and show the highest cytotoxic activity after compound **1**, although the aniline region involves different groups (4-NO_2, 2-OCH_3, and 2-Cl). Compound **1** possesses 3-OC_2H_5-4-OH substituents at the aldehydic region and exhibits the highest cytotoxic activity.

3.3 | Metabolic enzymes inhibition results

3.3.1 | Antidiabetic potential

In the study, the antidiabetic potential of novel thiosemicarbazones derivatives (**1–11**) were measured via α-Gly inhibition experiments. The results are presented in Table 2. These novel thiosemicarbazones derivatives (**1–11**) effectively inhibited α-Gly with K_i values in the range of 122.15 ± 16.80 to 333.61 ± 57.08 nM. All of these novel thiosemicarbazones derivatives (**1–11**) had almost similar inhibition profiles. The most active **6** showed K_i value of 122.15 ± 16.80 nM. For α-Gly, IC_{50} values of ACR as positive control and some novel compounds were studied in this study the following order: ACR (71.84 nM, r^2: 0.9162) <**6** (125.37 nM, r^2: 0.9371) <**7** (150.34 nM, r^2: 0.9277) <**5** (154.23 nM, r^2: 0.9724) <**8** (159.33 nM, r^2: 0.9105) <**4** (182.14 nM, r^2: 0.9360) < **11** (200.04 nM, r^2: 0.9683) <**2** (205.31 nM, r^2: 0.9437) <**10** (219.20 nM, r^2: 0.9572) <**3** (244.35 nM, r^2: 0.9481) <**1** (284.28 nM, r^2: 0.9153) <**9** (290.14 nM, r^2: 0.9989).

TABLE 2 The enzyme inhibition results of novel compounds (**1–11**) against acetylcholinesterase (AChE) and α-glycosidase (α-Gly) enzymes

Compounds	IC_{50} (nM)			K_i (nM)		
	AChE	r^2	α-Gly	r^2	AChE	α-Gly
1	11.05	0.9823	284.28	0.9153	7.37 ± 1.25	302.18 ± 26.54
2	15.34	0.9903	205.31	0.9437	12.35 ± 0.93	237.24 ± 50.31
3	10.13	0.9672	244.35	0.9481	12.35 ± 2.35	231.57 ± 24.62
4	3.43	0.9348	182.14	0.9360	3.04 ± 0.38	204.32 ± 23.05
5	3.11	0.9384	154.23	0.9724	3.01 ± 0.77	143.65 ± 43.71
6	2.17	0.9902	125.37	0.9371	1.93 ± 0.22	122.15 ± 16.80
7	2.91	0.9681	150.34	0.9277	2.15 ± 0.50	135.82 ± 37.88
8	3.01	0.9427	159.33	0.9105	3.45 ± 0.91	177.43 ± 13.36
9	9.14	0.9284	290.14	0.9989	6.97 ± 1.04	333.61 ± 57.08
10	14.23	0.9180	219.20	0.9572	12.36 ± 1.23	203.41 ± 35.76
11	9.34	0.9902	200.04	0.9683	8.40 ± 0.80	189.13 ± 22.52
TAC[a]	18.21	0.9237	–	–	17.45 ± 3.60	–
ACR[b]	–	–	71.84	0.9162	–	75.48 ± 8.31

Abbreviation: IC_{50}, half-maximal inhibitory concentration.

[a]Tacrine (TAC) was used as a standard inhibitor for AChE enzyme.

[b]Acarbose (ACR) was used as a positive control for α-Gly enzyme.

TABLE 3 The calculated docking score (DS), van der Waals energy (Evdw), coulomb energy (E Coul), Glide ligand efficiency (E Gle), and Glide energy (E Gle) between (**1 and 11**) drug candidates and selected target proteins for antiproliferative activity

	MCF-7 (1M17)					MDA-MB-231 (5FI2)				
	DS[a]	E vdw[a]	E Coul[a]	E Gle[a]	E Gli[a]	DS[a]	E vdw[a]	E Coul[a]	E Gle[a]	E Gli[a]
1	−7.582	−45.168	−13.415	−1.853	−51.398	−4.355	−26.847	−13.759	−0.207	−39.871
2	−5.229	−34.401	−3.562	−1.349	−39.730	−3.386	−28.225	−2.768	−0.147	−32.883
3	−5.136	−38.699	−3.572	−1.337	−40.448	−3.956	−30.750	−8.537	−0.165	−33.659
4	−5.819	−37.983	−3.206	−1.522	−44.905	−4.034	−25.019	−9.965	−0.176	−34.643
5	−6.624	−45.322	−9.803	−1.764	−48.724	−4.194	−24.771	−11.238	−0.185	−39.278
6	−6.460	−37.936	−7.459	−1.649	−48.543	−4.061	−24.677	−10.431	−0.184	−38.073
7	−7.154	−44.266	−12.498	−1.748	−49.808	−4.337	−27.520	−12.645	−0.200	−39.492
8	−5.587	−35.950	−5.301	−1.619	−44.578	−4.037	−25.122	−9.668	−0.181	−35.054
9	−4.518	−38.278	−3.004	−1.276	−39.515	−2.999	−29.440	−2.133	−0.120	−32.939
10	−4.464	−33.389	−0.100	−1.351	−39.210	−3.747	−27.520	−6.829	−0.163	−32.939
11	−5.384	−36.511	−3.221	−1.562	−44.204	−4.047	−26.957	−10.552	−0.183	−35.568
cis-Pt	−5.719	−35.695	−3.658	−1.402	−44.825	−3.993	−26.019	−8.745	−0.175	−33.632

[a]Unit is kcal/mol.

3.3.2 | Anti-Alzheimer potential

The inhibition impacts of thiosemicarbazones derivatives, which aimed to determine its biological activity potential, on AChE enzyme that is related with AD was studied in different concentrations and IC_{50} values were calculated. For evaluation of the effect of thiosemicarbazones on the indicated metabolic enzyme, the following results had been found. As can be seen from the results obtained in Table 2, these novel thiosemicarbazones derivatives (**1–11**) effectively inhibited AChE, with K_i values in the range of 1.93 ± 0.22 to 12.36 ± 1.23 nM. All of these novel thiosemicarbazones derivatives (**1–11**) had almost similar inhibition profiles. The most active **6**

TABLE 4 The calculated docking score (DS), van der Waals energy (Evdw), coulomb energy (E Coul), Glide ligand efficiency (E Gle), and Glide energy (E Gle) between (**1 and 11**) drug candidates and selected target proteins for enzyme inhibition effect

	AChE (4EY6)					α-Gly (4J5T)				
	DS[a]	E vdw[a]	E Coul[a]	E Gle[a]	E Gli[a]	DS[a]	E vdw[a]	E Coul[a]	E Gle[a]	E Gli[a]
1	−7.380	−41.372	−6.002	−0.351	−49.887	−3.743	−15.981	−9.486	−0.133	−22.466
2	−6.382	−44.226	−4.324	−0.255	−49.763	−3.927	−16.761	−10.186	−0.157	−23.946
3	−7.509	−43.936	−6.060	−0.341	−50.305	−3.905	−17.300	−10.180	−0.142	−22.480
4	−8.257	−44.142	−7.155	−0.393	−50.927	−4.440	−21.263	−9.364	−0.200	−30.627
5	−8.395	−45.656	−7.182	−0.382	−51.065	−4.717	−19.373	−14.492	−0.201	−33.865
6	−8.936	−43.578	−9.892	−0.406	−52.811	−4.931	−19.464	−18.922	−0.287	−38.386
7	−8.442	−43.827	−7.810	−0.352	−51.952	−4.832	−21.681	−12.968	−0.210	−34.649
8	−8.570	−42.189	−9.693	−0.408	−52.081	−4.468	−16.426	−11.057	−0.203	−27.483
9	−7.871	−46.364	−6.608	−0.328	−50.760	−3.734	−15.096	−4.887	−0.127	−19.982
10	−7.152	−46.602	−5.537	−0.311	−47.591	−3.745	−17.976	−9.788	−0.156	−21.764
11	−7.566	−40.983	−6.369	−0.329	−50.314	−4.171	−17.356	−8.430	−0.190	−25.785
TAC	−6.336	−45.032	−4.219	−0.225	−49.778	–	–	–	–	–
ACR	–	–	–	–	–	−4.698	−15.268	−28.921	−0.107	−44.189

Abbreviations: AChE, acetylcholinesterase; ACR, acarbose; TAC, tacrine; α-Gly, α-glycosidase.
[a]Unit is kcal/mol.

showed K_i values of 1.93 ± 0.22 nM. For AChE, IC_{50} values of tacrine (TAC) as positive control and some novel compounds were studied in this study the following order: **6** (2.17 nM, r^2: 0.9902) <**7** (2.91 nM, r^2: 0.9681) <**8** (3.01 nM, r^2: 0.9427) <**5** (3.11 nM, r^2: 0.9384) <**4** (3.43 nM, r^2: 0.9348) <**9** (9.14 nM, r^2: 0.9284) <**11** (9.34 nM, r^2: 0.9902) <**3** (10.13 nM, r^2: 0.9672) <**1** (11.05 nM, r^2: 0.9823) <**10** (14.23 nM, r^2: 0.9180) <**2** (15.34 nM, r^2: 0.9903) <TAC (18.21 nM, r^2: 0.9237).

3.4 | Molecular docking studies

Molecular docking results which are docking score (DS), van der Waals energy (Evdw), coulomb energy (E Coul), Glide ligand efficiency (E Gle), and Glide energy (E Gle) for selected drug candidates between (**1**–**11**) and PDB ID: 1M17 and 5FI2 for anticancer activity and PDB ID: 4EY6 and 4J5T for enzyme inhibition effect are given in Tables 3 and 4, respectively.

First, the selected proteins were subjected to receptor grid processing to identify the active sites. With the LigPrep step, the ligands were optimized. Optimized ligands were docked into proteins. The analyzed DS, Evdw, E Coul, E Gle, and E Gle parameters are directly related to the activity.[43] DS and E Gle are the two most important parameters that predict the interaction strength of the protein with the investigated ligand. The increasing value of these parameters is directly proportional to the increase in biological activity. It also exhibits a similar trend in other parameters studied. As with the experimental results, in terms of the propensity for antiproliferative activity, all compounds (**1**–**11**) are more active with the 1M17 target protein than 5FI2. In terms of enzyme inhibition efficiency, interactions with the 4EY6 target protein are more effective than 4J5T. Besides this, the trend between ligands obtained in docking results is highly consistent with the experimental trend. The DS of the **1**, **7,** and **5** compounds with the lowest IC_{50} values against the MCF-7 cell line were calculated −7.582, −7.154, and −6.460 kcal/mol, respectively. The activity tendency in other compounds differs from experimental only in compounds **2**, **3,** and **9**, **10**. IC_{50} values obtained against the MDA-MB-231 cell line were consistent with docking results. A similar situation is valid for enzyme inhibition activity, namely the experimental and computational results are compatible. This is even valid for reference compounds.

The results can be evaluated in terms of the substituent effect of molecular structures. The 3,5-diOCH_3-4-OH substituent significantly reduces the activity of compounds except those containing fluorine. If the evaluation is continued in terms of the halogen effect, it should not be ignored that compounds containing bromine increase biological activity. Electron withdrawing methoxy and hydroxyl group in *ortho*-position in compound **1** may have caused resonance hybrid formation in the π system in the ring. Thus, the substituent may have been induced and caused the mesomeric effect as an electron donor. Similarly, the presence of electron donor groups in the R and R_1 groups in compound **7** may have increased the activity. As a result, the activity of drug active ingredients may increase with the presence of electron-donor substrates. In the synthesis of similar compounds, it may be suggested to add donor groups to the skeletal structure. Finally, types of interactions between ligands and target proteins

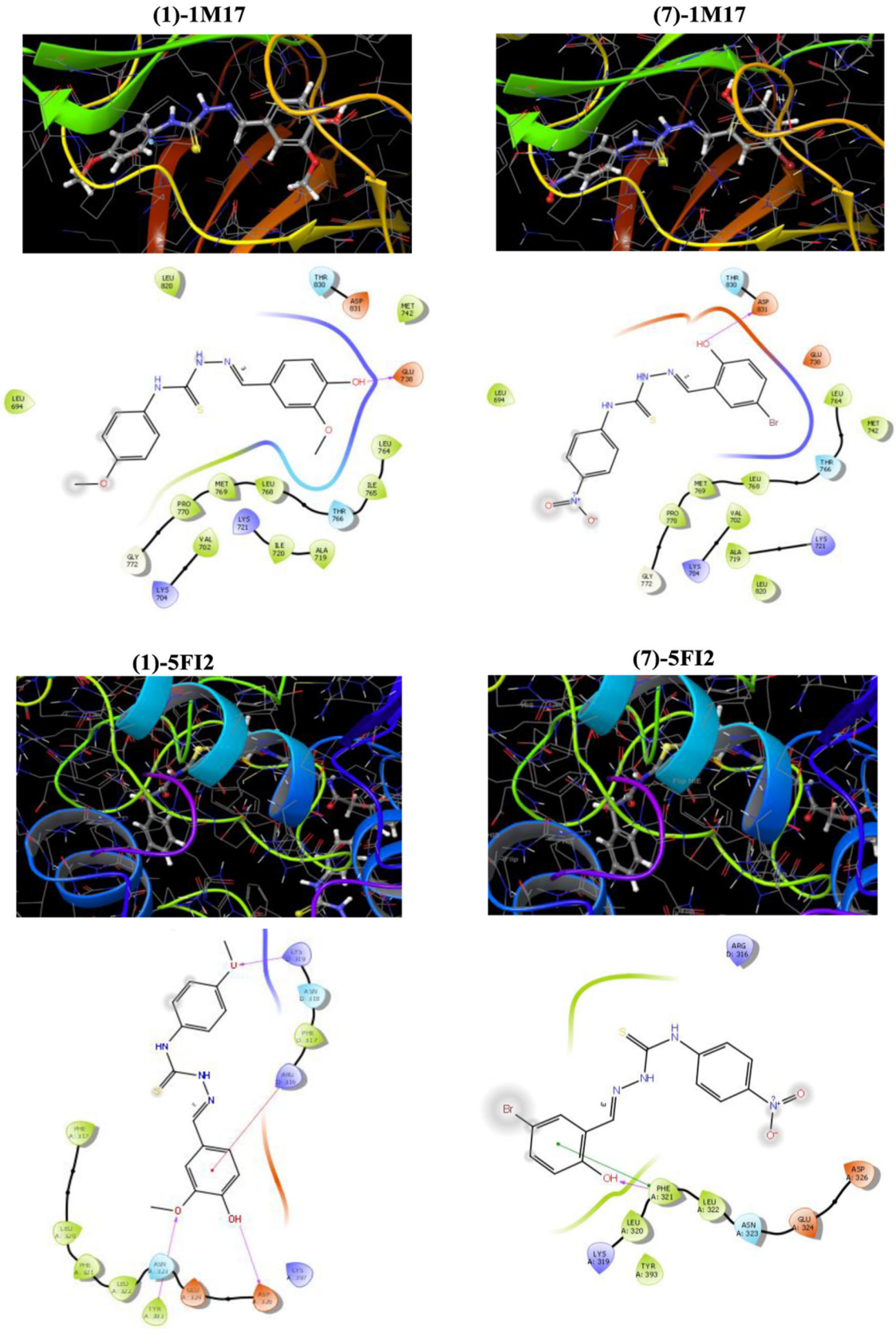

FIGURE 1 Docking pose and interaction of compounds **1** and **7** with target proteins

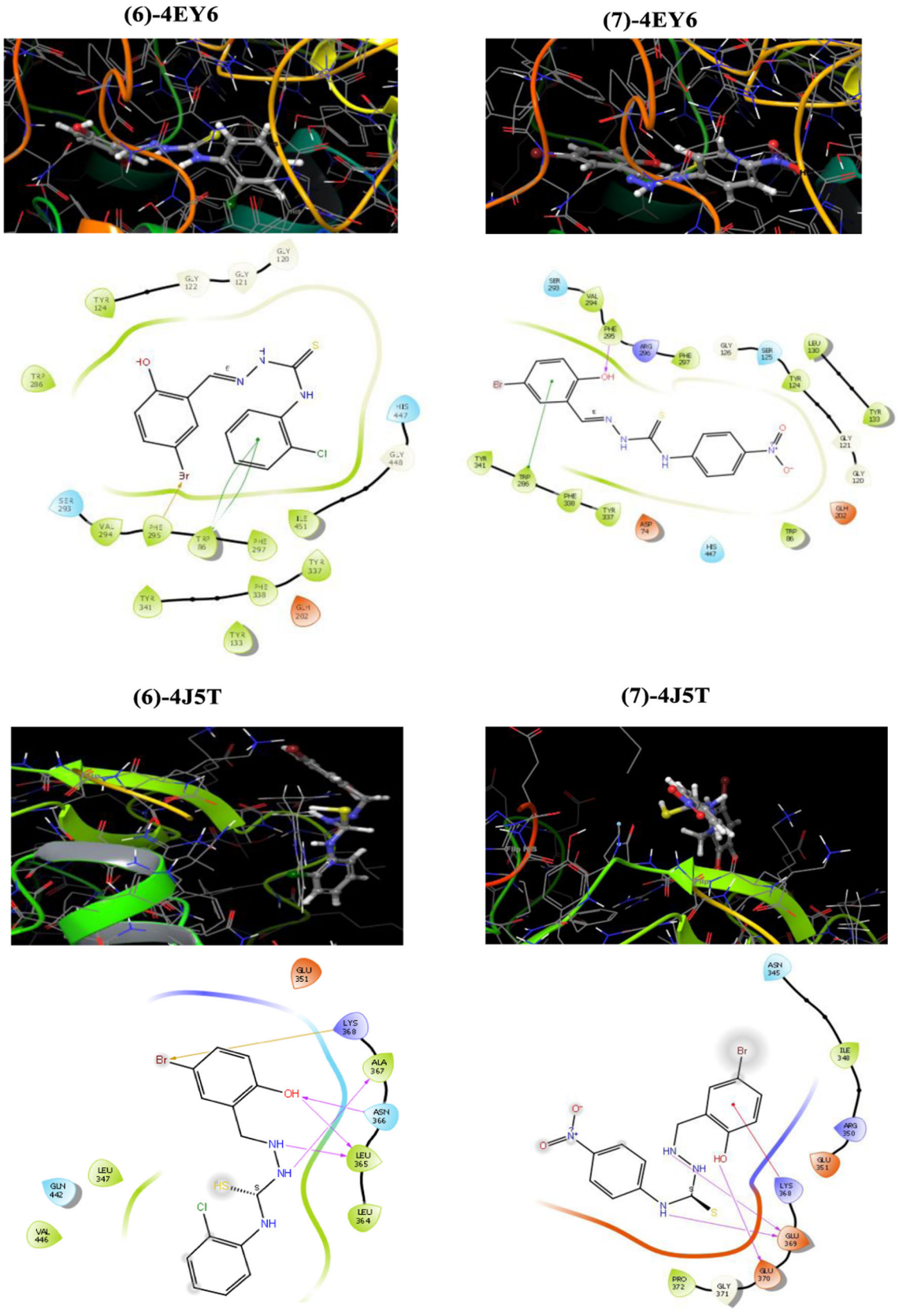

FIGURE 2 Docking pose and interaction of compounds **6** and **7** with target proteins

with high inhibitory efficiency were examined. Interaction types and bonding poses of complex structures with the highest antiproliferative activity and metabolic enzyme inhibition effects are given in Figures 1 and 2, respectively.

Our docking study showed that ligands bind to target proteins. H-bond was formed between the hydroxyl bound to the aldehydic site of 1 ligand and the GLU738 amino acid residue in 1M17. In this complex structure, amino acid residues PRO770 and VAL702 are in hydrophobic interaction between the ligand and the target protein. Also, it formed polar interactions with THR766 and THR830. The interaction types in compound **7** and 1M17, H-bonding, hydrophobic and polar interactions were observed as in compound **1**. ASP831 and LEU764, LEU768, MET769, PRO770, VAL702, and THR766 amino acid radiuses are played a role in H-bond, hydrophobic and polar, respectively. H-bonding, polar and hydrophobic interaction occurred between the 5FI2 target protein and cCompounds **1** and **7**. Compound **1** linked ASP326 and the TYR303 amino acid residue with the target protein 5FI2, unlike compound **7**, which linked PHE321 amino acid residue in target protein 5FI2. The more H-bonds between the Compound **1** ligand and the target protein may have increased the interaction energy. The interaction types number increased in enzyme inhibition activities according to the types of interactions observed in anticancer activities. Halogen bond and pi–pi interactions were also observed in the investigated enzyme inhibition interaction types. Compounds **6** and **7** formed an H-bond with the PHE295 amino acid residue of the 4EY6 target protein. Compound **6** is in polar interaction with TRP85 with pi–pi and SER293 with HIS447. H-bond (ASN366, LEU365, and ALA367) polar (GLN442), hydrophobic (LU347, LEU364, and VAL446), and halogen (LYS368) interactions from drug candidates (**6**) were observed with the 4J5T target protein. Compound **7** interacted with less interacting amino acid residue than the 6-4J5T complex structure.

4 | CONCLUSION

Herewith, novel thiosemicarbazone derivatives (**1**–**11**) including Schiff base were synthesized and isolated with good yields of 60–88%. The chemical structures of the obtained compounds were characterized by FT-IR, ^{1}HNMR, and ^{13}CNMR spectroscopy and elemental analysis. Cytotoxicity studies have shown that compound **1** has a remarkable cytotoxic effect in both MCF-7 and MDA-MB-231 cells, with IC_{50} values of 2.97 µM and 6.57 µM, respectively. The study also examined the potential of new thiosemicarbazone-based anticholinergic and antidiabetic compounds to be used as drugs, which can be an alternative to drugs that are in use and have a wide range of potential side effects. For this purpose, the effect of these newly synthesized thiosemicarbazone derivatives on AChE and α-Gly enzyme activities was measured spectrophotometrically. In contrast to used standard inhibitors, these compounds demonstrated high inhibitory activities with K_i values in the range of 122.15–333.61 nM for α-Gly (K_i value for standard inhibitor = 75.48 nM), 1.93–12.36 nM for AChE (K_i value for standard inhibitor = 17.45 nM). Molecular docking studies showed that the biological activities calculated with the experimental results were consistent with the DS of the target proteins and ligands. Overall, these newly synthesized thiosemicarbazone derivatives are potential metabolic enzyme inhibitors and anticancer agents.

ACKNOWLEDGMENT

This study was supported by the Scientific Research Project Fund of Sivas Cumhuriyet University (Project Number: RGD-020 and ECZ-079).

CONFLICT OF INTERESTS

The authors declare no conflict of interest.

AUTHOR CONTRIBUTIONS

Hasan Yakan: Writing–review, characterization, and supervision. **Ümit M. Koçyiğit:** Biological activity studies and supervision. **Halit Muğlu:** Synthesis and characterization. **Mustafa Ergul:** Cytotoxic studies. **Sultan Erkan:** Molecular docking studies. **Emre Güzel**: Characterization, writing – review, visualization, and editing. **Parham Taslimi:** Biological activity studies. **İlhami Gülçin:** Critical revision.

DATA AVAILABILITY STATEMENT

The data that support the findings of this study are available from the corresponding author upon reasonable request.

ORCID

Hasan Yakan http://orcid.org/0000-0002-4428-4696
Ümit M. Koçyiğit http://orcid.org/0000-0001-8710-2912
Halit Muğlu http://orcid.org/0000-0001-8306-2378
Mustafa Ergul http://orcid.org/0000-0003-4303-2996
Sultan Erkan http://orcid.org/0000-0001-6744-929X
Emre Güzel http://orcid.org/0000-0002-1142-3936
Parham Taslimi http://orcid.org/0000-0002-3171-0633
İlhami Gülçin http://orcid.org/0000-0001-5993-1668

PEER REVIEW

The peer review history for this article is available at https://publons.com/publon/10.1002/jbt.23018

REFERENCES

[1] H. Govender, C. Mocktar, H. M. Kumalo, N. A. Koorbanally, *Phosphorus, Sulfur Silicon Relat. Elem.* **2019**, *194*, 1074.
[2] S. A. Khan, P. Kumar, R. Joshi, P. F. Iqbal, K. Saleem, *Eur. J. Med. Chem.* **2008**, *43*, 2029.
[3] A. Sîrbu, O. Palamarciuc, M. V. Babak, J. M. Lim, K. Ohui, E. A. Enyedy, S. Shova, D. Darvasiová, P. Rapta, W. H. Ang, V. B. Arion, *Dalt. Trans.* **2017**, *46*, 3833.
[4] H. Muğlu, *Res. Chem. Intermed.* **2020**, *46*, 2083.
[5] H. Muğlu, H. Yakan, T. K. Bakir, *Turkish J. Chem.* **2020**, *44*, 237.
[6] M. M. Aly, Y. A. Mohamed, K. A. M. El-Bayouki, W. M. Basyouni, S. Y. Abbas, *Eur. J. Med. Chem.* **2010**, *45*, 3365.
[7] L. Labanauskas, V. Kalcas, E. Udrenaite, P. Gaidelis, A. Brukštus, V. Daukšas, *Pharmazie* **2001**, *56*, 617.
[8] T. P. Stanojkovic, D. Kovala-Demertzi, A. Primikyri, I. Garcia-Santos, A. Castineiras, Z. Juranic, M. A. Demertzis, *J. Inorg. Biochem.* **2010**, *104*, 467.

[9] V. F. S. Pape, S. Tóth, A. Füredi, K. Szebényi, A. Lovrics, P. Szabó, M. Wiese, G. Szakács, *Eur. J. Med. Chem.* **2016**, *117*, 335.
[10] D. Sriram, P. Yogeeswari, R. Thirumurugan, R. K. Pavana, *J. Med. Chem.* **2006**, *49*, 3448.
[11] S. Eğlence-Bakır, O. Sacan, M. Şahin, R. Yanardag, B. Ülküseven, *J. Mol. Struct.* **2019**, *1194*, 35.
[12] Y. Qin, R. Xing, S. Liu, K. Li, X. Meng, R. Li, J. Cui, B. Li, P. Li, *Carbohydr. Polym.* **2012**, *87*, 2664.
[13] L. N. de Araújo Neto, M. do Carmo Alves de Lima, J. F. de Oliveira, E. R. de Souza, M. D. S. Buonafina, M. N. Vitor Anjos, F. A. Brayner, L. C. Alves, R. P. Neves, F. J. B. Mendonça-Junior, *Chem.–Biol. Interact.* **2017**, *272*, 172.
[14] Ü. M. Koçyiğit, H. Gezegen, P. Taslimi, *Arch. Pharm.***2020**, *353*, 2000202.
[15] T. Arslan, N. Çakır, T. Keleş, Z. Biyiklioglu, M. Senturk, *Bioorg. Chem.* **2019**, *90*, 103100.
[16] E. Güzel, F. Sönmez, S. Erkan, K. Çıkrıkçı, A. Ergün, N. Gençer, O. Arslan, M. B. Koçak, *Turkish J. Chem.* **2020**, *44*, 1565.
[17] F. A. Larik, M. S. Shah, A. Saeed, H. S. Shah, P. A. Channar, M. Bolte, J. Iqbal, *Int. J. Biol. Macromol.* **2018**, *116*, 144.
[18] S. A. R. B. Rombouts, F. Barkhof, C. S. Van Meel, P. Scheltens, *J. Neurol., Neurosurg. Psychiatry* **2002**, *73*, 665.
[19] F. Türkan, Z. Huyut, P. Taslimi, M. T. Huyut, İ. Gülçin, *Drug Chem. Toxicol.* **2020**, *43*, 423.
[20] F. A. Larik, A. Saeed, M. Faisal, S. Hamdani, F. Jabeen, P. A. Channar, A. Mumtaz, I. Khan, M. A. Kazi, Q. Abbas, M. Hassan, J. Korabecny, S. Y. Seo, *J. Mol. Struct.* **2020**, *1203*, 127459.
[21] R. Ujan, A. Saeed, P. Channar, F. Larik, Q. Abbas, M. Alajmi, H. El-Seedi, M. Rind, M. Hassan, H. Raza, S. Y. Seo, *Molecule* **2019**, *24*, 860.
[22] Y. J. Shim, H. K. Doo, S. Y. Ahn, Y. S. Kim, J. K. Seong, I. S. Park, B. H. Min, *J. Ethnopharmacol.* **2003**, *85*, 283.
[23] M. H. Mehraban, M. Motovali-Bashi, Y. Ghasemi, *Biochem. Biophys. Res. Commun.* **2019**, *519*, 192.
[24] Y. Demir, P. Taslimi, Ü. M. Koçyiğit, M. Akkuş, M. S. Özaslan, H. E. Duran, Y. Budak, B. Tüzün, M. B. Gürdere, M. Ceylan, S. Taysi, İ. Gülçin, Ş. Beydemir, *Arch. Pharm.***2020**, *353*, e2000118.
[25] S. Bezabeh Kassa, P. Taslimi, Ş. Özel, B. Gür, İ. Gülçin, Onganer. *Colloids and Surfaces A: Physicochemical and Engineering*, Vol. 632, Elsevier, **2020**.
[26] L. K. Campbell, D. E. Baker, R. K. Campbell, *Ann. Pharmacother.* **2000**, *34*, 1291.
[27] B. Tüzün, *Turkish Comput. Theor. Chem.* **2020**, *4*, 76.
[28] M. Ergul, F. Bakar-Ates, *Anticancer Agents Med. Chem.* **2019**, *19*, 1846.
[29] Ü. M. Koçyiğit, P. Taslimi, B. Tüzün, H. Yakan, H. Muğlu, E. Güzel, *J. Biomol. Struct. Dyn.* **2020**. https://doi.org/10.1080/07391102.2020.1857842
[30] M. Boztaş, Y. Çetinkaya, M. Topal, I. Gülçin, A. Menzek, E. Şahin, M. Tanc, C. T. Supuran, *J. Med. Chem.* **2015**, *58*, 640.
[31] G. L. Ellman, K. D. Courtney, V. Andres, R. M. Featherstone, *Biochem. Pharmacol.* **1961**, *7*, 88.
[32] H. Genç Bilgiçli, A. Kestane, P. Taslimi, O. Karabay, A. Bytyqi-Damoni, M. Zengin, İ. Gulçin, *Bioorg. Chem.* **2019**, *88*, 102931. https://doi.org/10.1016/j.bioorg.2019.102931
[33] K. Sayin, A. Üngördü, *Spectrochim. Acta—Part A Mol. Biomol. Spectrosc.* **2019**, *220*, 117102.
[34] J. Stamos, M. X. Sliwkowski, C. Eigenbrot, *J. Biol. Chem.* **2002**, *277*, 46265.
[35] L. A. McDermott, P. Iyer, L. Vernetti, S. Rimer, J. Sun, M. Boby, T. Yang, M. Fioravanti, J. O'Neill, L. Wang, D. Drakes, W. Katt, Q. Huang, R. Cerione, *Bioorg. Med. Chem.* **2016**, *24*, 1819.
[36] S. A. Güngör, M. Tümer, M. Köse, S. Erkan, *J. Mol. Struct.* **2020**, *1206*, 127780.
[37] U.M. Kocyigit, *Fresen Envıron Bull.* **2019**, 2739.
[38] H. Yakan, *Res. Chem. Intermed.* **2020**, *46*, 3979.
[39] W. X. Hu, W. Zhou, C. N. Xia, X. Wen, *Bioorg. Med. Chem. Lett.* **2006**, *16*, 2213.
[40] T. R. Bal, B. Anand, P. Yogeeswari, D. Sriram, *Bioorg. Med. Chem. Lett.* **2005**, *15*, 4451.
[41] A. Hameed, K. M. Khan, S. T. Zehra, R. Ahmed, Z. Shafiq, S. M. Bakht, M. Yaqub, M. Hussain, A. De La Vega De León, N. Furtmann, J. Bajorath, H. A. Shad, M. N. Tahir, J. Iqbal, *Bioorg. Chem.* **2015**, *61*, 51.
[42] M. Islam, A. Khan, M. T. Shehzad, A. Hameed, N. Ahmed, S. A. Halim, M. Khiat, M. U. Anwar, J. Hussain, R. Csuk, Z. Shafiq, A. Al-Harrasi, *Bioorg. Chem.* **2019**, *87*, 155.
[43] S. Vijayakumar, P. Manogar, S. Prabhu, R. A. Sanjeevkumar Singh, *J. Pharm. Anal.* **2018**, *8*, 413.

SUPPORTING INFORMATION

Additional supporting information may be found in the online version of the article at the publisher's website.

How to cite this article: H. Yakan, Ü. M. Koçyiğit, H. Muğlu, M. Ergul, S. Erkan, E. Güzel, P. Taslimi, İ. Gülçin, *J. Biochem. Mol. Toxicol.* **2022**;36:e23018. https://doi.org/10.1002/jbt.23018